

# A revised alpha-ejection correction calculation for (U-Th)/He thermochronology dates of broken apatite crystals

John J. Y. He<sup>1</sup>, Peter W. Reiners<sup>1,2</sup>

<sup>1</sup>Department of Geoscience, University of Arizona, Tucson, AZ, 85721, USA

5 <sup>2</sup>Faculty of the Environment, University of Northern British Columbia, Prince George, BC V2N 4Z9, Canada

*Correspondence to:* John He (johnhe@email.arizona.edu)

**Abstract.** Accurate corrections for the effects of alpha ejection (the loss of daughter He near grain or crystal surfaces due to long alpha-stopping distances) is central to (U-Th)/He thermochronometry. In the case of apatite (U-Th)/He dating, alpha-ejection correction is complicated by the fact that crystals are often broken perpendicular to the c-axis. In such cases the correction should account for the fact that only some parts of the crystal are affected by alpha-ejection. A common current practice to account for such broken crystals is to modify measured lengths of broken crystals missing one termination by a factor of 1.5, and those missing both terminations by a factor of 2. This alpha-ejection “correction correction” systematically overestimates the actual fraction of helium lost to alpha ejection, and thus overcorrects the measured date relative to that determined for an otherwise equivalent unbroken crystal. The alpha-ejection-affected surface-area-to-volume ratio of a fragmented crystal is equivalent to the surface-area-to-volume ratio of an unbroken crystal twice as long (for fragments with one termination), and equivalent to that of an unbroken crystal infinitely long (for fragments with no termination). We suggest it is appropriate to revise the fragmentation correction to multiply the length of crystals missing one c-axis termination by 2, and those missing both c-axis termination by some large number  $> \sim 20$ , respectively. We examine the effect of this revised correction and demonstrate the accuracy of the new method using synthetic datasets. Taking into account alpha-ejection, rounding of the He concentration profile due to diffusive loss, and accumulation of radiation damage over a range of thermal histories, we show that the revised fragmentation alpha-ejection correction proposed here accurately approximates the corrected date of an unbroken crystal (“true” date) to within  $< 0.7\%$  on average ( $\pm 4.2\%$ ,  $1\sigma$ ), whereas the former method overcorrects dates to be  $\sim 3\%$  older than the “true” date, on average. For individual grains, the former method can result in older dates by a few percent in most cases, and by as much as 12% for grains with aspect ratio of up to 1:1. The revised alpha-ejection correction proposed here is both more accurate and more precise than the previous correction, and does not introduce any significant systematic bias to the apparent dates from a sample.

## 1 Introduction

Since the development of modern apatite (U-Th)/He thermochronometry, the technique has become a versatile and powerful tool for a range of geological problems (Zeitler et al. 1987; Farley *et al.*, 1996; Flowers et al., 2022, a, b). To fully leverage the power of the technique, however, it is necessary to account for the wide range of possible complications that commonly cause data dispersion greater than analytical errors. Of particular significance is correcting for the loss of daughter nuclides due to the problem of alpha ejection. Apatite He dating uses the accumulation of daughter nuclide  $^4\text{He}$  (i.e., alpha particles) from the spontaneous alpha decay of  $^{238}\text{U}$ ,  $^{235}\text{U}$ , and  $^{232}\text{Th}$  (as well as a minor contribution from  $^{147}\text{Sm}$ ) to constrain possible thermal histories of samples, which is sometimes simplified as providing a date of cooling through some closure temperature ( $\sim 30\text{-}90$  °C) at which helium diffusion out of a crystal is sufficiently slow for the system to be considered closed. However, this method is complicated by the fact that the sizes of most typical apatite crystals are only several times greater than the stopping distance of alpha particles ( $\sim 20$   $\mu\text{m}$ ), meaning that the fraction of  $^4\text{He}$  ejected from a crystal must be accounted for in most applications (Farley *et al.*, 1996).

Careful measurement of crystal geometries allows accurate approximation of the cumulative alpha-ejection loss of helium from a crystal (Ziegler; 1977; Farley *et al.*, 1996; Farley, 2002; Hourigan et al. 2005; Ketcham et al. 2011; Reiners *et al.*, 2018). Because the likelihood of an alpha particle being ejected from a crystal is directly related to a parent nuclide's proximity to the crystal surface, the fraction of helium retained in the crystal ( $F_T$ ) is a function of a crystal's surface area to volume ratio ( $\beta$ ) (Farley *et al.*, 1996). In the simplest case of a spherical grain with homogenous parent nuclide distribution,  $F_T$  is a cubic polynomial function of  $\beta$  (Farley *et al.*, 1996).  $F_T$  can be estimated for other geometries using a polynomial function calibrated by Monte Carlo alpha-ejection models (Farley, 2002; Ketcham et al, 2011). In practice, a parent-nuclide-specific  $F_T^i$  is determined and a corrected date can be calculated by incorporating it into the full decay equation:

$$^4\text{He} = 8(^{238}\text{U})(F_T^{238})(e^{\lambda_{238}t} - 1) + 7(^{235}\text{U})(F_T^{235})(e^{\lambda_{235}t} - 1) + 6(^{232}\text{Th})(F_T^{232})(e^{\lambda_{232}t} - 1) + (^{147}\text{Sm})(F_T^{147})(e^{\lambda_{147}t} - 1)$$

[Eq. 1]

where  $t$  is the unknown variable that must be solved numerically or iteratively;  $^4\text{He}$ ,  $^{238}\text{U}$ ,  $^{235}\text{U}$ ,  $^{232}\text{Th}$ , and  $^{147}\text{Sm}$  contents are measured;  $\lambda_i$  is the decay constant for the given isotope;  $F_T^i$ , the alpha-ejection correction factor for the given isotope calculated from crystal geometry (Ketcham *et al.*, 2011). A more approximate corrected date can also be calculated by simply dividing the measured (raw) date by  $F_T$  (Farley and Stockli, 2002), though this is less accurate for older dates.

Deleted: in pres

Deleted: s

Deleted: both

70 These calculations generally assume the ideal case of a euhedral, prismatic crystal with homogenous parent nuclide distribution, entire original crystal faces, and insignificant parent nuclide concentrations outside and within one alpha-stopping distance of the exterior of the crystal during the interval in which temperature was low enough to accumulate He. When these assumptions are violated, further adjustments to the standard  $F_T$  correction are required.

75 If information about the magnitude and pattern of parent-nuclide zonation is available, an adjusted  $F_T$  may be applied to account for inhomogeneous parent-nuclide distribution (Hourigan *et al.*, 2005, Farley *et al.*, 2011, Ault and Flowers, 2012, Gautheron *et al.*, 2012). Absent such information, as is the case in most routine analyses, use of the standard unzoned correction assuming homogenous distribution of the parent nuclide would introduce errors that skew a crystal's apparent date to be younger, if its rim is enriched in parent nuclides, and older if it is depleted in parent nuclides (Farley *et al.*, 1996; Hourigan *et al.*, 2005). For apatite, these errors are usually minor (<1.5% for 80% of apatite crystals, and <9.5% for 80 95%), because apatite crystals in most cases do not typically exhibit extreme zonation of parent nuclides (Ault and Flowers, 2011, [in the case of old cratonic samples](#)). [The data from that study suggests that](#) the errors are usually symmetrically distributed, with apatite populations not exhibiting bias towards either rim-enriched or rim-depleted grains, [though this may not be the case for those from rocks that experienced metamorphism or hydrothermal alteration](#). Accounting for effects of He implantation from sources external to the grains is not typically possible for grains separated from their petrographic context, although in some cases particular date-eU ([effective uranium concentration](#)) or date-Rs ([sphere equivalent radius](#)) correlations may be used to interpret such effects (Spiegel *et al.*, 2009; Murray *et al.*, 2014).

90 The focus of this paper is the adjustment to the  $F_T$  correction that should be made in the case of crystals that are broken perpendicular to the c-axis, as common for apatite, [whether during mineral separation or during erosion and transport \(if the fragmentation occurred recent relative to the timing of cooling\)](#). If errors due to fragmentation are large, they can significantly impede our ability to extract geologically meaningful information from dates calculated from parent-daughter nuclide ratios. Broken and [morphologically](#) suboptimal crystals are frequently analyzed, particularly when the quality of mineral separates is poor and/or the apatite yield from a sample is low. In addition, imperfect basal (0001) cleavage in apatite (Dana, 1963; Palache *et al.*, 1963) leads to the fact that many dated crystals are broken 95 perpendicular to their c-axis and lack original terminations, even for high-quality samples. [A](#) common strategy is to apply a fragmentation correction to the  $F_T$ -calculation, which accounts for the fact that the fracture exposes surface area where alpha ejection did not occur (Farley, 2002). This correction seeks to be approximately correct for the originally greater length of the unbroken apatite crystal, by multiplying the length of all broken crystals by 1.5 (if one end is broken) or 2 (if both ends are broken) (Farley, 2002; 100 Farley *et al.*, 1996; Brown *et al.*, 2013; Beucher *et al.*, 2013; Reiners *et al.*, 2018). Though it is not possible

Deleted: Furthermore,

Deleted: (Ault and Flowers, 201

Deleted: 1)

Deleted: size

Deleted: Assuming that fragmentation occurred recently relative to the date measured (e.g. during mineral separation, or in the case of detrital samples, during recent transport), a

110 to find the original length of broken crystals, Farley (2002) argued that these approximations are sufficient because  $F_T$  is relatively insensitive to the length of the crystal.

115 An alternative approach to this problem is that of Brown et al. (2013), who argued that, for interpreting thermal histories, it is best to leave dates uncorrected and instead evaluate the variation in date among crystals with different morphologies and numbers of broken ends. If one assumes that breakage occurred prior to cooling to temperatures of partial He retention, raw (uncorrected) dates of broken crystals can vary by up to 60% for certain t-T histories, and that for sufficiently large datasets of fragmented crystals, considering the patterns of dispersion in uncorrected dates can constrain thermal history (Brown et al. 2013). In practice, however,  $F_T$ -corrected dates remain widely reported, partly because correcting for alpha ejection and fragmentation is necessary to compare dates to other datasets and dates of geologic significance. A more accurate correction would allow both broken and unbroken crystals within a sample and across samples to be appropriately compared without introducing additional systematic bias.

120 Although the conventional fragmentation correction has been widely applied, its accuracy and precision has not been demonstrated. In the first part of this paper, we consider the rationale behind the early approach, then propose a revision and compare the results of both methods. We test the new method using synthetic data and demonstrate the accuracy of the revised correction. We take into account a range of broken crystal sizes, number of terminations present, and various thermal histories and their associated effects on helium diffusivity, and we quantify the uncertainty that can be attributed to the fragmentation correction alone. Considering the numerous natural sources of uncertainty in apatite He dating, achieving greater confidence in the accuracy of the fragmentation  $F_T$  correction and minimizing its uncertainty ultimately aids in the interpretation of other possible sources of uncertainty and errors (He et al., 2021).

130

## 2. Revision of $F_T$ correction for broken crystals

For an idealized spherical grain, the alpha-ejection correction is a function of the radius of the sphere ( $R$ ) and the alpha stopping distance for the given parent nuclide ( $S$ ):

$$F_T = 1 - \frac{3S}{4R} + \frac{S^3}{16R^3}$$

135

[Eq. 2]

(Farley et al., 1996). Where  $R \gg S$ , the function approaches a linear relationship:

$$F_T = 1 - \frac{3S}{4R} \quad \text{or,} \quad F_T = 1 - \frac{S\beta}{4}$$

[Eq. 3]

Deleted: since the widespread application of the technique

Deleted: then

Formatted: Font:Italic

Formatted: Font:Italic

Formatted: Font:Italic

Formatted: Font:Italic

(Farley et al., 1996), where  $\beta$  is the ratio of surface area of a crystal to its volume. In other words, the fraction of helium lost due to alpha ejection near the crystal surface is approximately a function of the ratio of surface area of a crystal to its volume. Considering more realistic crystal geometries, polynomial equations that define the  $F_T^i$  value as a function of  $\beta$  have been empirically determined using Monte Carlo simulations for each parent nuclide  $i$  and their respective alpha stopping distance (Farley et al., 1996; Hourigan et al., 2005). For hexagonal prisms, simply measuring the length ( $L$ ) and radius or half-width of the cylindrical prism ( $R$ ) allows the computation of  $\beta$ :

$$\beta = \frac{2R + (4/\sqrt{3})L}{LR}$$

[Eq. 4]

- 150 The general idea behind modified  $F_T$  corrections is to modify  $\beta$ , under the assumption that the polynomial functions relating  $\beta$  and  $F_T$  are nearly identical for similar geometries (e.g., hexagonal prism with bipyramidal or pinacoidal terminations). This was the approach taken to correct for lost crystal surface in the case of crystals polished parallel to the c-axis (Reiners et al., 2007). In the case of c-axis perpendicular breakage, the Farley et al. (1996) approach sought to establish the length of the original, unbroken crystal.
- 155 Because it was observed that the corrected-length-to-radius ratios of most apatite crystals (5:1) were sufficiently high such that the  $F_T$  corrections become largely independent of length, it became standard practice at most laboratories to simply modify  $\beta$  by multiplying the lengths of broken crystals by arbitrary factors of 1.5 or 2, thereby modifying  $F_T$  (Farley et al. 1996; Farley, 2002). Alternatively, in the slightly different context of inverse modelling a large set of uncorrected ages, Beucher et al. (2013) suggested
- 160 that a rule of thumb for predicting the unknown initial length should be to add the maximum fragment length of a set of fragments and two times the maximum radius. To the first order, guessing the unknown initial length using consistent factors such as these suffices to roughly account for the loss of alpha-ejection-affected surface area at the tips: this is because as  $L$  increases, the increase in surface area of a crystal is less than that of the volume, in effect reducing  $\beta$ .
- 165 In detail, however, the fraction of helium remaining in a fragmented crystal does not depend on the unknown (and precisely unknowable) initial length. Rather, it should be directly related to the surface area of a broken crystal that was originally affected by alpha-ejection. Assuming that we can identify when crystals have lost one or both terminations, that the breakage generally occurs more than one average-alpha-stopping-distance from the tip, and that diffusion has not significantly modified the
- 170 daughter concentration profiles, the alpha-ejection-affected-surface-area-to-volume ratio ( $\beta_a$ ) could be simply calculated by measuring and then subtracting the surface area of the broken face(s) from the total surface area. For a hexagonal prism, simple geometric calculations demonstrate that the  $\beta_a$  of singly and doubly broken crystals are equivalent to the  $\beta$  of an unbroken crystal of the same width that is twice as

Formatted: Font:Italic

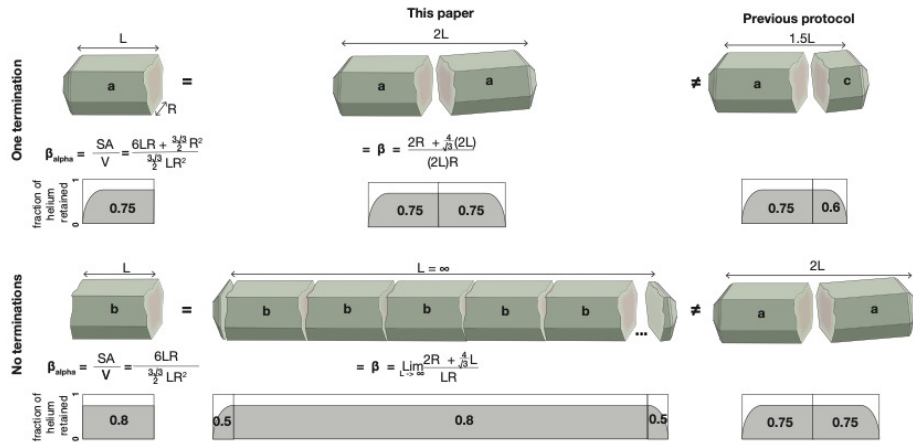
Formatted: Font:Italic

Deleted: +2R

Deleted: but arbitrary poorly-known

long, or infinitely long, respectively; this is shown graphically in Fig. 1. Consider that the helium profile in an unbroken crystal is symmetrical such that when broken in half, each half will have the same fraction of helium remaining ( $F_T$ ); thus, conversely, any broken crystal with one termination (breakage occurring more than one alpha-stopping distance from the tip) has the same  $F_T$  as a hypothetical unbroken crystal double its length (but not the same as the original unbroken crystal). For crystals with no terminations remaining, any c-axis perpendicular segment or cross section of the crystal will have the same  $F_T$ , no matter its length or its position along the fragment; therefore fragments with no terminations have the same  $F_T$  as an infinitely long unbroken crystal, where the terminations, which have a different  $F_T$ , have a vanishingly small effect on the overall  $F_T$  of the crystal.

185



190

Fig. 1. The alpha-ejection-affected surface-area-to-volume ratio, or  $\beta_{\alpha}$ , of a broken crystal that has lost a basal fragment longer than one alpha-stopping distance is equivalent to the surface-area-to-volume ratio of an unbroken crystal twice as long (for fragments with one termination), and equivalent to that of an unbroken crystal infinitely long (for fragments with no termination). The simple geometric calculations shown assume a flat hexagonal termination, but apply by the same logic to any geometry, regardless of the shape of its body (e.g. cylindrical, tetragonal, or hexagonal) or the shape of its terminations (e.g. pyramidal, flat, or rounded). The profiles of fraction of helium retained that are shown below each fragment are schematic and serve only to illustrate the equivalence or non-equivalence of fragments of different lengths (e.g. a = 0.75, b = 0.8, c = 0.75), and do not correspond to any specific dimensions. As discussed in text, these calculations assume no change to the daughter concentration profile due to diffusion.

195

**Deleted:**

**Formatted:** Font color: Text 1

**Deleted:** This assumes that the fragment is broken more than one average-alpha-stopping-distance from the tip,

**Deleted:** and ignores

**Deleted:** any

It follows, then, that a more accurate fragmentation correction that explicitly considers the lost surface area of a broken crystal should be to multiply the length of a broken crystal by 2 or some large number (to simulate the limit as L approaches infinity), respectively, rather than 1.5 or 2, i.e.:

$$\beta_a = \frac{2R + (8/\sqrt{3})L}{2LR} \quad \text{for crystals broken on one end; and}$$

$$\beta_a = \lim_{L \rightarrow \infty} \frac{2R + 4/\sqrt{3}L}{LR} \quad \text{for crystals broken on both end}$$

where L is the measurement of the crystal dimension perpendicular to the fracture (since crystals commonly break perpendicular to the c-axis in apatite crystals, L should usually be measured parallel to the c-axis, even if it is shorter than the width). In the unlikely case of an oblique fragment, L should be the average of the longer and shorter sides. This simple correction has the benefit of applying to other geometries, regardless of the shape of its body (e.g. cylindrical, tetragonal, or hexagonal) or the shape of its terminations (e.g. pyramidal, flat, or rounded): the  $\beta_a$  of any singly broken crystal is equivalent to the  $\beta$  of a whole crystal twice its length, and the  $\beta_a$  of any doubly broken crystal is equivalent to the  $\beta$  of a whole crystal infinitely long. The correction can thus be applied to all crystals broken perpendicular to the c-axis, regardless of original length, requiring knowledge of only the width and length of the broken crystal, and the number of terminations present. Similarly, this correction can be applied to zircon fragments (though it is uncommon to see zircon fragments with only one termination or no terminations).

We emphasize that though this fragmentation correction is similar in form to that of Farley (2002) in that it involves length-modifying factors, it differs in that it seeks to approximate the length of a whole crystal with the same fraction of helium remaining as the fraction remaining in the broken fragment, rather than seeking to approximate the unknown length of the original unbroken crystal.

Deleted: +2R

[Eq. 5]

Formatted: Right

Deleted: +2R

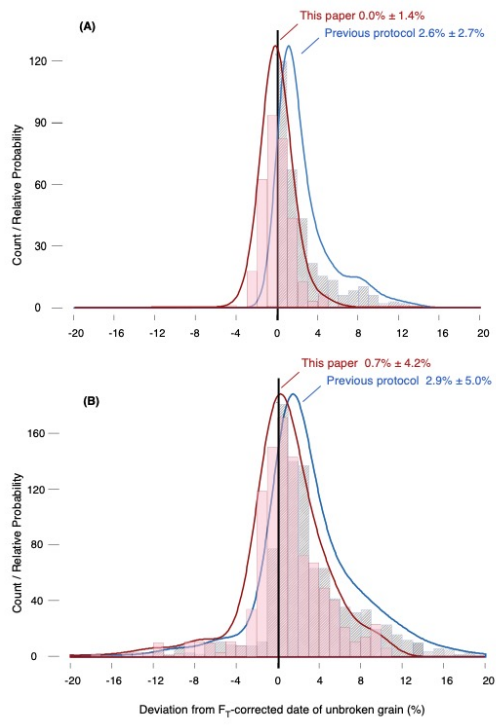
Deleted: s

[Eq. 6]

Formatted: Right

Deleted: )

Deleted: .



230 Fig. 2. Histograms and kernel density estimate (KDE) functions comparing the new protocol suggested in this paper (red) and the  
 235 previous protocol (blue), as applied to a synthetic dataset of raw, uncorrected dates ( $n=1000$ , cf. Brown et al., 2013). The error is  
 defined to be the % deviation of the  $F_T$ -corrected dates of a broken crystal from the  $F_T$ -corrected date of the whole crystal, which is  
 known because the synthetic fragments are generated from a whole crystal with a known “age”. The new protocol is more accurate  
 and more precise at correcting for the effect of fragmentation, both in the ideal case (A) assuming that fragmentation has occurred  
 more than one average-alpha-stopping-distance from the tip, and that there is no significant diffusive modification of the helium  
 profile, as well as in the more realistic scenario (B) when these assumptions are relaxed. In other words, (B) includes corrected dates  
 from fragments that are broken close to the tip, and fragments that experienced thermal histories leading to significant diffusive  
 modification, in addition to the dates contained in (A). Annotations show the mean  $\pm$  standard deviation ( $1\sigma$ ); KDE functions are  
 normalized to the same peak height.

240



### 3. Accuracy and precision of the revised $F_T$ correction

To characterize the uncertainty of the new and old protocols, we applied the above fragmentation correction equations to a synthetic dataset of raw (uncorrected) dates of broken prismatic crystals where the corrected dates of the original unbroken crystals are known. Note that as a simplification, a length-modifying factor of 20 is used to approximate the limit to infinity (see Section 4.1). For comparable results between the new and old protocol, we used the same datasets of raw uncorrected dates from Brown *et al.* (2013), which are generated from the volume-integrated  $^4\text{He}$  concentration in a random set of crystal fragments broken at varying positions along the original crystal (Beucher *et al.* 2013). We assume uniform spatial distribution of the parent nuclide, and apply both protocols to all fragments exactly as we would calculate  $F_T$  corrected dates in routine laboratory analyses: i.e. we assume no knowledge of the original length and thermal history of the crystals to compute the corrected age, and use only the raw date, length and width of the broken crystals, and the number of terminations present for the calculation. We then compare the  $F_T$ -corrected dates of the synthetic fragments with the known  $F_T$ -corrected date of the corresponding unbroken crystals. These original unbroken crystals from which the fragments were generated have a constant geometry (hexagonal prism that is 400  $\mu\text{m}$  long and 150  $\mu\text{m}$  wide), and experienced one of five different representative thermal histories (rapid monotonic cooling; slow monotonic cooling; prolonged isothermal residence in the partial retention zone followed by rapid cooling; a mix of slow cooling and isothermal holding in the partial retention zone; and gradual reheating (e.g. burial) followed by rapid cooling; cf. Wolf *et al.* 1998).

To test the accuracy of the proposed protocol under the stated ideal assumptions (that the fragmentation has occurred more than one average-alpha-stopping-distance from the tip, and that there is no significant diffusion-induced modification of the helium concentration profile), we excluded any randomly generated crystals broken  $<20 \mu\text{m}$  from the tip, and included only fragment sets that experienced the two thermal histories (monotonic cooling) associated with the least amount of diffusive modification of the helium profile (Fig. 2a). To approximate the actual circumstances under which fragments are analyzed in laboratories, where we have no a priori knowledge of the thermal history and cannot readily discern where a crystal has broken, we included the full fragment dataset (Fig. 2b). 23% of the randomly generated fragments in that dataset were broken within  $\sim 20 \mu\text{m}$  from the tip, and 60% experienced complex thermal histories involving reheating or extended residence in the partial retention zone.

The new protocol accurately corrects for the effect of fragmentation, deviating by  $0.0\% \pm 1.4\%$  ( $1\sigma$ ) from the corrected date of the unbroken crystal, under the ideal assumptions stated above (Fig. 2a). By comparison, under the same assumptions, the old protocol leads to corrected dates that are almost all too old, on average by  $2.6\% \pm 2.7\%$ . When the two assumptions are relaxed, the proposed fragmentation correction results in a broader range of uncertainty ( $+0.7\% \pm 4.2\%$ ), but it is nevertheless more accurate

**Moved down [1]:** The new protocol accurately corrects for the effect of fragmentation, deviating by  $0.0\% \pm 1.4\%$  ( $1\sigma$ ) from the corrected date of the unbroken crystal, under the ideal assumptions stated above: that the fragmentation has occurred more than one average-alpha-stopping-distance from the tip, and that there is no significant diffusion-induced modification of the helium concentration profile (Fig. 2a). By comparison, under the same assumptions, the old protocol leads to corrected dates that are almost all too old, on average by  $2.6\% \pm 2.7\%$ .

**Deleted:** .  
**Deleted:** Characterization of the uncertainty for both protocols is based on

**Deleted:** the application of the  
**Deleted:** protocols

**Deleted:** Note that as a simplification, a length-modifying factor of 20 is used to approximate the limit to infinity (see Section 4.1).  
**Deleted:** ,

**Deleted:** that are

**Moved (insertion) [2]**

**Deleted:** These results are based on the full fragment dataset from Brown *et al.*, 2013, which includes a representative range of thermal histories that are more complicated than simple rapid cooling (i.e. slow, monotonic cooling; prolonged isothermal residence in the partial retention zone followed by rapid cooling; a mix of slow cooling and isothermal holding in the partial retention zone; and gradual reheating (e.g. burial) followed by rapid cooling; cf. Wolf *et al.* 1998).

**Deleted:** , accounting for the possibility that in real laboratory analyses, it is not always discernible whether an apatite crystal was broken more than an alpha-stopping distance from the tip. Thus, our application of the two  $F_T$  corrections to the full dataset in Fig. 2b approximates the actual circumstances under which broken crystals are analyzed.

**Moved (insertion) [1]**

**Deleted:** : that the fragmentation has occurred more than one average-alpha-stopping-distance from the tip, and that there is no significant diffusion-induced modification of the helium concentration profile

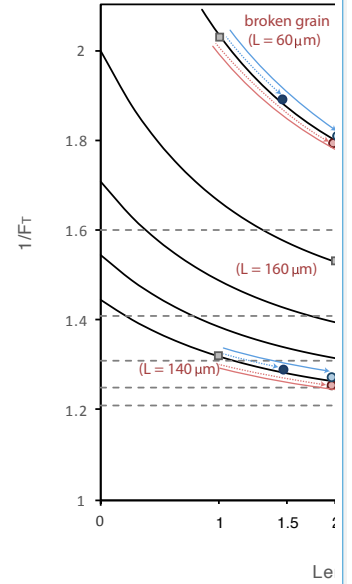
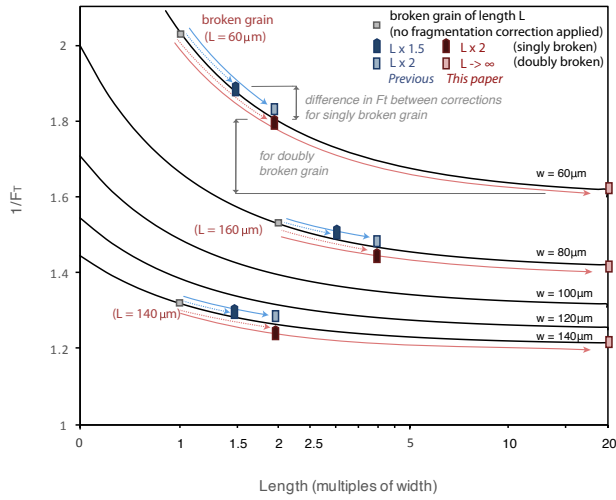
**Deleted:** .

**Deleted:** In a more realistic scenario,

**Deleted:** w

315 and more precise than the old protocol ( $+2.9\% \pm 5.0\%$ ) (Fig. 2b). Using the new protocol, only 3% of  
 320 corrected dates deviate from the corrected date of the unbroken crystal by greater than 10%; this  
 represents a 66% reduction relative to the prior protocol.

**Moved up [2]:** These results are based on the full fragment dataset from Brown et al., 2013, which includes a representative range of thermal histories that are more complicated than simple rapid cooling (i.e. slow, monotonic cooling; prolonged isothermal residence in the partial retention zone followed by rapid cooling; a mix of slow cooling and isothermal holding in the partial retention zone; and gradual reheating (e.g. burial) followed by rapid cooling; cf. Wolf et al. 1998). 23% of the randomly generated fragments in that dataset were broken within  $\sim 20\mu\text{m}$  from the tip, accounting for the possibility that in real laboratory analyses, it is not always discernible whether an apatite crystal was broken more than an alpha-stopping distance from the tip. Thus, our application of the two  $F_T$  corrections to the full dataset in Fig. 2b approximates the actual circumstances under which broken crystals are analyzed.



325 Fig. 3. The inverse of  $F_T$  value plotted as a function of crystal length  $L$ , as used in the calculation of  $\beta$  or  $\beta_w$ . For a broken crystal,  
 this is measured parallel to the c-axis (as a multiple of width), and modified by some factor (see legend). The inverse of  $F_T$  can be  
 approximately considered a multiplier for the raw date, where corrected date  $\approx$  raw date  $\times (1/F_T)$  (Farley et al., 1996). Inverse  $F_T$   
 330 corrections for three example fragments are shown (width = 60, 80, and 140  $\mu\text{m}$ , and length = 60, 160, and 140, respectively), with  
 the corresponding fragment-corrected  $F_T$  values for singly- or doubly-broken crystals. The gray squares indicate the actual length  
 of the fragment, and show their inverse  $F_T$  values if no fragmentation correction is applied. For convenience, the asymptotic value  
 is assumed to be approximately the same as multiplying by some large number (e.g., 20). Note that strictly speaking, calculation of  
 a corrected date requires using the full decay equation with an individual  $F_T^L$  for each nuclide, rather than the simplification of  
 corrected date  $\approx$  raw date  $\times (1/F_T)$ .

**Deleted:**  
**Formatted:** Font color: Text 1  
**Deleted:** Dashed lines indicate the asymptote for  $\lim_{L \rightarrow \infty}$ .  
**Deleted:** , plotted at the edge of the graph (open red circle)

## 4.1. Difference between corrections for different crystal dimensions

Though multiplying a fragment length by different factors may seem to be a minor revision, the resulting difference in corrected dates is not negligible. This is partly because the [observation](#) that  $F_T$  corrections [is not strongly dependent](#) on length, upon which the fragmentation correction was initially based, does not hold true for the smaller crystals commonly analyzed today (e.g., c-axis perpendicular width < 150 $\mu$ m). Fig. 3 shows the effect of crystal length (or modified crystal length, as used in the calculation of  $\beta$  or  $\beta_a$ ) on the inverse value of  $F_T$ , an approximation for the correction's effect on the final reported date (Fig. 3). Since both protocols effectively multiply the length of a broken crystal to compute an adjusted  $F_T$  value, the inverse  $F_T$  values of the new and old protocols for any given crystal width all lie on the same curve for  $F_T$  as a function of length (normalized to width). Particularly when the length of a broken crystal is close to its width, and when the width is small, the  $F_T$  correction is not independent of the modified length. For example, for a singly-broken crystal that is 60  $\mu$ m in width and equally long (the minimum dimensions of crystals routinely analyzed in our lab), the difference between the new and old protocols, would be 4%; for a doubly-broken crystal of the same dimensions, the difference would be 12% (Fig. 4).

The overcorrection of the previous protocol could be even larger for drum-shaped fragments (i.e. crystals broken on both ends, and shorter in c-axis-parallel length than width). For a broken crystal that is 140  $\mu$ m in both width and length, the difference would be 2% and 5% (for singly and doubly-broken crystals, respectively). The magnitude of these differences is not negligible, at least relative to other sources of error in  $F_T$  corrections. By comparison, for example, the updated alpha-ejection models of Ketcham *et al.* (2011) based on revised alpha-stopping distances affects dates by approximately 1-5%, and 2D measurement of crystal geometry introduces errors of  $\sim$ 2% (Cooperdock *et al.*, 2019).

Deleted: presumption

Deleted: does not

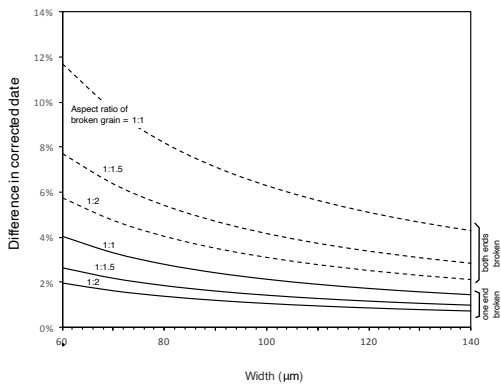


Fig. 4. Difference between the corrected date calculated from the standard protocol and revised protocol (Dashed—broken on both ends; Solid—broken on one end), shown for a range width-to-length ratios commonly seen in broken crystals.

380

#### 4.2. Uncertainty in fragmentation correction compared to other sources of date dispersion

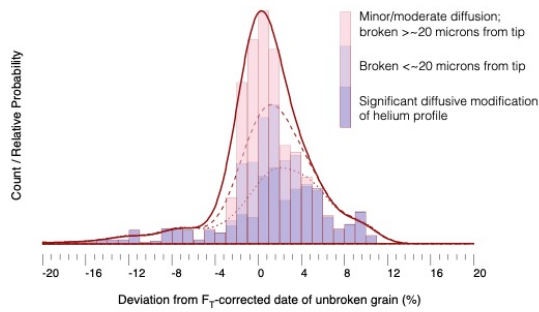
In the ideal case (that the fragmentation has occurred more than one average-alpha-stopping-distance from the tip, and that there is no significant diffusion-induced modification of the helium concentration profile), we have shown that the proposed fragmentation correction is both accurate and precise ( $\pm < 1.4\%$ ). When these ideal assumptions are relaxed, the uncertainty increases ( $\pm < 4.2\%$ ) (Fig. 2b). The larger uncertainties are largely due to the diffusive modification of helium profiles. In our test of this protocol, all cases of corrected fragment dates that deviate by more than  $> 5\%$  from the corrected date of the unbroken crystal can be attributable to thermal histories involving prolonged residence in the partial retention zone (Fig. 5). Without a priori knowledge of a sample's thermal history, this is a problem for the new fragmentation correction just as it is for the old protocol, because the calculation of  $F_T$  correction only assumes loss of helium due to alpha ejection. The additional uncertainty associated with the fragmentation correction fundamentally relates to the fact that using  $\beta_\alpha$  to correct  $F_T$  implies taking the

385

390

**Deleted:** in the fragmentation correction with the two ideal assumptions relaxed (Fig. 2b)

395 lost surface area (“skin”) affected by alpha ejection as a proxy for the lost volume (the outer “shell”) of  
the crystal affected by alpha ejection.

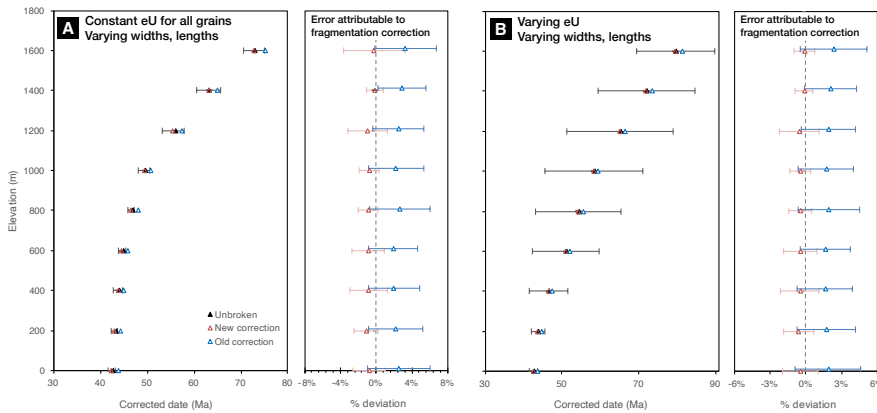


400 **Fig. 5. Uncertainty associated with the proposed fragmentation correction due to inclusion of fragments broken too close to the tip (dashed) and due to thermal histories that involve significant diffusive modification of the helium profile (dotted). The histogram and curves are stacked and cumulative, such that the dashed probability curve includes both close-to-tip fragments as well as fragments with significant diffusive loss.**

We emphasize that because the  $F_T$ -corrected dates of the fragments are compared to the  $F_T$ -corrected date of a whole crystal, Fig. 2 and Fig. 5 assesses only the effect of brokenness correction alone. **Parent-nuclide**  
405 **zonation**, eU variation, and diffusive helium loss remain important sources of additional error and dispersion (e.g. Meesters and Dunai, 2002; Herman et al., 2007, Gautheron et al 2012, Brown et al., 2013; Beucher et al., 2013). Notwithstanding the effects of date variation due to all these effects, the fragmentation correction proposed in this paper more consistently and accurately reproduces the  $F_T$ -corrected date of unbroken crystal. An illustrative case is that of a hypothetical date-elevation transect  
410 from a crustal block that cooled slowly through the partial retention zone until some point in time, then subsequently experienced very rapid cooling (from Brown et al., 2013). A key observation of Brown et al. (2013) was that the large dispersion of raw uncorrected fragment dates is due to the fact that these dates can be both younger and older than the whole crystal, and that fragments of same length can yield different dates, while conversely, fragments of different lengths can yield the same date. The dispersion  
415 is compounded because slow cooling leads to significant diffusive modification of the helium profile in a crystal. Despite this large dispersion of uncorrected fragment dates (up to 60%), and despite variations in eU and grain sizes, applying the new fragmentation correction introduces limited uncertainty relative to the dispersion caused by other effects (Fig. 6). This facilitates interpretation of widely-dispersed data

420 by reducing the number of variables that must be considered, and demonstrates the utility of applying a fragmentation correction when analysis of the pattern of dispersion in >20-30 crystals is not practical. Finally, while both the new and old  $F_T$  correction for broken crystals reliably approximates the corrected date of an unbroken crystal for a range of eU and crystal sizes, the new correction reduces the systematic bias that is introduced by the old protocol when many broken crystals are analyzed in a sample by ~3-4% (Fig. 6).

425



430 Fig. 6. a) Date-elevation transect of a crustal block that cooled slowly through the partially retention zone, and was subsequently rapidly exhumed (cf. Brown et al. 2013, Fig. 9), showing fragment dates corrected using the new protocol (red), compared to previous protocol (blue), and the expected whole-crystal date (black). Note that the red and black triangles may be difficult to distinguish because they overlap in most cases. Corrected dates are from fragments of varying lengths, both singly and doubly broken, generated from crystals with variable widths and lengths, but constant eU. Error bars in date-elevation transect represent intra-sample date dispersion and are shown for the new protocol only. Error bars in the right panel show the % deviation of the corrected fragment dates from their corresponding corrected whole-crystal dates, using the new (red) and old protocol (blue). (b) Same as (a), but fragments were generated from crystals of varying eU (15-100 ppm, Brown et al., 2013), in addition to varying width and length. Notice that the introduction of eU as a variable significantly increased the intra-sample dispersion of corrected dates, but that the error attributable to the fragmentation correction alone was not materially affected. All error bars are  $1\sigma$ .

440 Ultimately, the characterization of the uncertainty due to the application of the fragmentation correction moves us one step closer to a more comprehensive quantification of all the uncertainty involved with apatite He dating (Fig. 7). Previous work has already shown, for example, that

- Deleted: nearly
- Deleted: all
- Deleted: Dispersion of corrected fragment dates
- Deleted: Right
- Deleted: shows
- Deleted: average
- Deleted: .
- Deleted: .
- Deleted: can be propagated with other sources of error (analytical, zonation, etc.), for appropriate comparison of fragment dates and other corrected dates where the correction was not applied.
- Moved down [3]: For larger datasets, especially in the case of larger-n analyses, this contributes to our understanding of the expected distribution of corrected dates from any given sample (Fig. 7) (He et al., 2021)
- Deleted: .

(1) size- and eU-dependent diffusivity can cause apparent dates to systematically vary (Reiners and Farley, 2001; Flowers et al. 2009; Whipp et al., 2022).

460 (2) The presence of extraneous daughter nuclides whose parent nuclides are not accounted for can cause outlier dates many multiples older than the true date (<sup>4</sup>He-rich fluid inclusions; U- or Th-rich inclusions or microinclusions where the inclusions are not fully dissolved; grain boundary phases or adjacent grains that contribute helium to the grain but are not in the analyzed aliquot) (Spiegel et al. 2009; Fitzgerald et al. 2006; Murray et al. 2014).

465 (3) Non-uniform distribution of the parent nuclides (i.e., "zonation") can cause dates to be both older or younger by  $\leq 1.5\%$  in most cases. Even if zonations are not accounted for, the probability distribution of errors due to zonations can be approximated by either examining a representative selection of apatite in a sample, or using a reference compilation (e.g. Ault and Flowers, 2011) (Fig. 7a).

470 (4) Technician-to-technician differences in 2D grain measurement cause date variations that differ from actual 3D geometry by  $\sim 2\%$ . (Cooperdock et al., 2019).

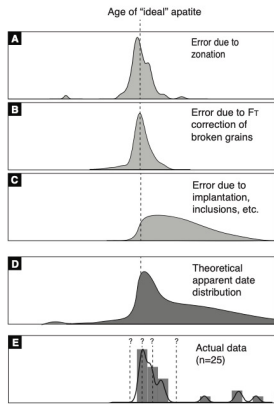
475 A future step towards a more rigorous evaluation of the uncertainty of individual-grain analyses or samples as a whole could involve the propagation of each of these uncertainties to account for sample and grain specific information such as the probability of implantation (approximated from the spatial distribution of heavy minerals in a sample, via X-Ray Computed Tomography), the probability of extreme parent nuclide zonations in a sample (based on fission track mounts) or from a reference compilation, and whether fragments were analyzed. The resulting distribution (e.g. Fig. 7d) would then represent the sample-specific probability of single-aliquot apatite He dates. For larger datasets, especially in the case of larger-n analyses (e.g. Fig. 7e), this would provide a more robust rationale for the interpretation of the geologically significant date. For smaller datasets, the expected distribution would inform our selection of the appropriate summary statistic to represent the date variation in a given sample (He et al., 2021).

Deleted: a few percent

Deleted: .

Formatted: Normal

Deleted: .



490 Fig. 7. Illustration of how uncertainties due to different complications in apatite helium dating, e.g. uncertainty due to zonation (a),  
 uncertainty due to correction for broken crystals (b), and error due to implantation and other effects (c) could together be combined  
 to form a theoretical apparent date distribution (d) that would inform our interpretation of real data and the choice of the  
 appropriate summary statistic (whether the minimum, mean, median, peak date) in representing a sample's date. Note that (a) is  
 based on actual data from Ault and Flowers (2011), (b) is based on this study, whereas (c) is schematic. The last panel (e) is a  
 representative sample (n=25) that shows the expected non-normal and right-skewed distribution from an actual large-n sample (He  
 et al., 2019; Thomson et al., 2019). The peak date in this case would likely approximate the date of an "ideal" apatite, but a full  
 495 accounting of the probability of various uncertainties would provide a more robust rationale for that interpretation.

Deleted: Schematic

Deleted: i

Deleted: (Ault and Flowers, 2011)

Deleted: , this study

Deleted: .

Deleted: errors

Deleted: .

### Section 4.3. Timing of fragmentation

500 Finally, we emphasize that whether or not to apply the fragmentation correction in the first place is a  
 decision that precedes the choice of the protocol. For non-detrital samples, any crystals with existing  
 fractures prior to cooling would most likely still be intact, from an alpha-ejection perspective (i.e. the  
 fragments are immediately adjacent, such that He is implanted across fractures). This means that the  
 fragmentation correction to a crystal that has lost one or two termination(s) would still need to be applied  
 even if a fracture was present before cooling. On the other hand, the question of when the fracture  
 occurred matters for He diffusion. Depending on the thermal history, and whether the fracture pathway  
 505 was a free surface for He loss, the He concentration profile of the fragment would be the result of some



515 combination of alpha ejection having acted on external non-fragmented surfaces and diffusion having acted on all free surfaces. An additional complication, for certain thermal histories (e.g. partially reset samples), is that a broken face that is still adjacent to the other broken side (so that it has not experienced alpha-ejection helium loss) may experience more diffusion at this fracture plane than the exposed external faces where diffusion is inhibited by the lower He concentration at the crystal boundary.

520 For detrital samples the situation is more complicated. The accuracy of the protocol proposed above, as with the previous fragmentation protocol, is founded upon the assumption that fragmentation occurred recently, relative to the timing of cooling. This is not always straightforward to assess. For samples such as modern river sands derived from crystalline rocks, an assumption that c-axis-perpendicular breakage occurred after cooling (approximately below the closure temperature) can be reasonably based on textural clues, particularly the contrast between detrital apatite grains that are rounded or abraded by transport and the sharp faces and corners of fragment surfaces that have not. For sedimentary samples that have not been clearly buried and reset, e.g. sedimentary rocks not buried more than couple km, the timing of fragmentation would be more ambiguous, unless the age of the deposition is known (assuming that the age of the deposition is close to the age of erosion and transport, and therefore the timing of fragmentation).

530 Analogous to problem of unknown timing of abrasion for rounded detrital apatite and zircon grains (Rahl et al., 2003; Thomson et al., 2013; Reiners et al., 2018), if the timing of fragmentation is unknown, we could define a maximum date  $A_{fc}$ , the F<sub>T</sub>-corrected date without fragmentation correction, corresponding to fragmentation before or immediately after cooling; and a minimum date  $A_{ffc}$ , the fully FT-corrected date with fragmentation correction, corresponding to fragmentation during laboratory mineral separation. If there is sufficient geologic context, we can take the date of the sediment  $A_s$  to be the latest time at which the fragmentation occurred, such that the minimum date,  $A_{min}$ , would instead be:

$$A_{min} = (A_{ffc}) + (A_{fc} - A_{ffc})(A_s / A_{fc})$$

[Eq. 7]

A conservative approach would then be to display a “plot date” that is the mean of the maximum and minimum possible dates, and an error bar depicting the possible range of dates (Thomson et al., 2013).

540 In the case of detrital samples for which the timing of fragmentation is unknown, and that have also experienced non-monotonic cooling so that there has been significant diffusive loss after fragmentation (e.g. a fragment in a sedimentary rock that has been partially reset by burial-induced heating), fragmentation-corrected dates will be systematically younger than the corrected dates of whole, unbroken grains. For example, the corrected dates of any whole crystal may reflect a date-Rs (sphere-equivalent radius) relationship, and naively applying the fragmentation correction to fragments will lead to corrected dates that all lie below this the corrected date-Rs relationship of unbroken crystals. In this case, a plot

550 date with a maximum and minimum date could still be calculated, as defined above. The plot dates would  
reflect a similar date- $R_s$  relationship: i.e. if fragmentation occurred soon after cooling and significantly  
before partial reheating, the maximum date  $A_{fc}$  would be the closest to the corrected date of an equivalent  
unbroken grain (except that it would be younger than the equivalent unbroken grain to the extent that the  
unbroken grain is less affected by diffusion due to its size). To consider the date-size relationship of  
555 fragments, it would be necessary to either calculate an assumed sphere-equivalent radius ( $R_s'$ ) using the  
half-width and an assumed aspect ratio for typical ratios, or to use a sphere-equivalent radius based on  $F_T$   
(cf. Cooperdock et al., 2019), using the fragment's alpha-ejection-affected- $F_T$  value proposed here. The  
rationale for the latter option would be analogous to the case of the fragmentation  $F_T$  correction: the alpha-  
ejection-affected surface-to-volume ratio of a broken crystal is a good proxy for the available-for-  
diffusion-surface-to-volume ratio.

560 In all cases where significant diffusive loss complicates the application of fragmentation correction, the  
best way to approach the problem may be to consider a combination of factors in deciding whether to  
apply the fragmentation correction or calculate a plot age that is combination of the fragment-corrected  
date and the normal  $F_T$ -corrected date: a.) whether the fragment-corrected dates are systematically  
younger than the corrected dates of unbroken grains, b.) whether there is geologic context to suspect  
earlier fragmentation, and c.) whether there is a date-size correlation of corrected dates of unbroken  
565 grains.

## 5. Conclusion

570 Despite the dispersion of raw (U-Th)/He dates due to fragmentation, it is possible to accurately correct  
for the effect of fragmentation based on basic measurements routinely recorded during the grain selection  
process. In compensating for the effects of alpha ejection in broken crystals, the  $F_T$  correction should be  
calculated by explicitly taking into account the surface area of the broken face, rather than by assuming  
the unknown length of the original unbroken crystal. In individual cases, especially crystals with smaller  
width or whose length is less than or around the same as the width, the difference in apparent dates  
calculated with the two methods can be 12% or greater.

575 We further applied both the previous and newly proposed protocol for correction of broken crystals to a  
synthetic dataset. Even taking into account the effects of diffusive loss of helium and breakage close to  
tips of crystals, the proposed protocol more accurately and more precisely approximates the  $F_T$ -corrected  
date of an unbroken crystal for a range of complex and simple thermal histories. For a crystal of 150  $\mu\text{m}$   
width, the old calculation leads to apparent dates that are on average 3% older than the corrected dates of

Moved (insertion) [3]

Deleted: For larger datasets, especially in the case of larger-n analyses, this contributes to our understanding of the expected distribution of corrected dates from any given sample (Fig. 7) (He et al., 2021 - ... [3])

unbroken crystals, and in [extreme cases, up to 20% \(e.g. for drum-shaped fragments with no terminations that experienced gradual reheating\)](#).

Deleted: certain

585

The proposed adjustment allows more accurate comparison of data between samples of varying quality, which is common when a mix of different rock types is sampled. The greatest effect will be for samples where the majority of crystals are broken. Though this adjustment is minor in many cases, when applied to entire datasets, it significantly reduces one common source of error in calculations of individual apparent dates, and removes an easily correctable source of systematic bias towards older dates.

590

#### **Code availability**

Kernel density plots were produced using DensityPlotter (<https://www.ucl.ac.uk/~ucfbpve/densityplotter/>)

#### **Data availability**

Individual corrected fragment dates can be found in the supplementary file, and are calculated using methods discussed in text and applied to the cited synthetic datasets.

595

#### **Author Contribution (CReDIT taxonomy)**

JH – Conceptualization, formal analysis, methodology, visualization, writing-original draft; PWR-Supervision, resources, methodology, writing-review and editing

#### **600 Competing Interests**

The authors declare they have no competing interests.

#### **References**

Ault, A. K. and Flowers, R. M.: Is apatite U–Th zonation information necessary for accurate interpretation of apatite (U–Th)/He thermochronometry data?, *Geochim. Cosmochim. Acta*, 79, 60–78, <https://doi.org/10.1016/j.gca.2011.11.037>, 2012.

605

- Beucher, R., Brown, R. W., Roper, S., Stuart, F., and Persano, C.: Natural age dispersion arising from the analysis of broken crystals: Part II. Practical application to apatite (U-Th)/He thermochronometry, *Geochim. Cosmochim. Acta*, 120, 395–416, <https://doi.org/10.1016/j.gca.2013.05.042>, 2013.
- 610 Brown, R. W., Beucher, R., Roper, S., Persano, C., Stuart, F., and Fitzgerald, P.: Natural age dispersion arising from the analysis of broken crystals. Part I: Theoretical basis and implications for the apatite (U-Th)/He thermochronometer, *Geochim. Cosmochim. Acta*, 122, 478–497, <https://doi.org/10.1016/j.gca.2013.05.041>, 2013.
- Cooperdock, E. H. G., Ketcham, R. A., and Stockli, D. F.: Resolving the effects of 2D versus 3D grain measurements on (U-Th)/He age data and reproducibility, *Geochronol. Discuss.*, 1–32, <https://doi.org/10.5194/gchron-2019-3>, 2019.
- 615 Dana, E. s.: *A Textbook on Mineralogy*, John Wiley, New York, 1963.
- Farley, K. A.: (U-Th)/He Dating: Techniques, Calibrations, and Applications, *Rev. Mineral. Geochemistry*, 47, 819–844, <https://doi.org/10.2138/rmg.2002.47.18>, 2002.
- 620 Farley, K. A. and Stockli, D. F.: (U-Th)/He Dating of Phosphates, *Rev. Mineral. Geochemistry*, 15, 559–577, <https://doi.org/10.2138/rmg.2002.48.15>, 2002.
- Farley, K. A., Wolf, R. A., and Silver, L. T.: The effects of long alpha-stopping distances on (U-Th)/He ages, *Geochim. Cosmochim. Acta*, 60, 4223–4229, [https://doi.org/10.1016/S0016-7037\(96\)00193-7](https://doi.org/10.1016/S0016-7037(96)00193-7), 1996.
- 625 Farley, K. A., Shuster, D. L., and Ketcham, R. A.: U and Th zonation in apatite observed by laser ablation ICPMS, and implications for the (U-Th)/He system, *Geochim. Cosmochim. Acta*, 75, 4515–4530, <https://doi.org/10.1016/j.gca.2011.05.020>, 2011.
- Fitzgerald, P. G., Baldwin, S. L., Webb, L. E., and O’Sullivan, P. B.: Interpretation of (U-Th)/He single grain ages from slowly cooled crustal terranes: A case study from the Transantarctic Mountains of southern Victoria Land, *Chem. Geol.*, 225, 91–120, <https://doi.org/10.1016/j.chemgeo.2005.09.001>, 2006.
- 630 Flowers, R. M., Ketcham, R. A., Shuster, D. L., and Farley, K. A.: Apatite (U-Th)/He thermochronometry using a radiation damage accumulation and annealing model, *Geochim. Cosmochim. Acta*, 73, 2347–2365, <https://doi.org/10.1016/j.gca.2009.01.015>, 2009.
- 635 Flowers, R. M., Zeitler, P. K., Danišik, M., Reiners, P. W., Gautheron, C., Ketcham, R. A., Metcalf, J. R., Stockli, D. F., Enkelmann, E., and Brown, R. W.: (U-Th)/He chronology: Part 1. Data, uncertainty, and reporting, *Geol. Soc. Am. Bull.*, 2022a, <https://doi.org/10.1130/B30919.1>.

Deleted: In press.

- Flowers, R. M., Ketcham, R. A., Enkelmann, E., Gautheron, C., Reiners, P. W., Metcalf, J. R., Danišik, M., Stockli, D. F., and Brown, R. W.: (U-Th)/He chronology: Part 2. Considerations for evaluating, integrating, and interpreting conventional individual aliquot data, *Geol. Soc. Am. Bull.*, 2022b.
- Gautheron, C., Tassan-Got, L., Ketcham, R. A., and Dobson, K. J.: Accounting for long alpha-particle stopping distances in (U-Th-Sm)/He geochronology: 3D modeling of diffusion, zoning, implantation, and abrasion, *Geochim. Cosmochim. Acta*, 96, 44–56, <https://doi.org/10.1016/j.gca.2012.08.016>, 2012.
- 645 He, J., Stuart N. Thomson, and Peter W. Reiners.: Apatite (U-Th)/He thermochronometric data show rapid late Eocene incision in the central Transantarctic Mountains, *AGU Fall Meeting Abstracts*, vol. 2019, C53B-1340, <https://ui.adsabs.harvard.edu/abs/2019AGUFM.C53B1340H/abstract>, 2019.
- He, J., Thomson, S. N., Reiners, P. W., Hemming, S. R., and Licht, K. J.: Rapid erosion of the central Transantarctic Mountains at the Eocene-Oligocene transition: Evidence from skewed (U-Th)/He date distributions near Beardmore Glacier, *Earth Planet. Sci. Lett.*, 567, 117009, <https://doi.org/10.1016/j.epsl.2021.117009>, 2021.
- Herman, F., Braun, J., Senden, T. J., and Dunlap, W. J.: (U-Th)/He thermochronometry: Mapping 3D geometry using micro-X-ray tomography and solving the associated production-diffusion equation, *Chem. Geol.*, 242, 126–136, <https://doi.org/10.1016/j.chemgeo.2007.03.009>, 2007.
- 655 Hourigan, J. K., Reiners, P. W., and Brandon, M. T.: U-Th zonation-dependent alpha-ejection in (U-Th)/He chronometry, *Geochim. Cosmochim. Acta*, 69, 3349–3365, <https://doi.org/10.1016/j.gca.2005.01.024>, 2005.
- Ketcham, R. A., Gautheron, C., and Tassan-Got, L.: Accounting for long alpha-particle stopping distances in (U-Th-Sm)/He geochronology: Refinement of the baseline case, *Geochim. Cosmochim. Acta*, 75, 7779–7791, <https://doi.org/10.1016/j.gca.2011.10.011>, 2011.
- 660 Meesters, A. G. C. A. and Dunai, T. J.: Solving the production-diffusion equation for finite diffusion domains of various shapes: Part I. Implications for low-temperature (U-Th)/He thermochronology, *Chem. Geol.*, 186, 333–344, 2002.
- Murray, K. E., Orme, D. A., and Reiners, P. W.: Effects of U-Th-rich grain boundary phases on apatite helium ages, *Chem. Geol.*, 390, 135–151, <https://doi.org/10.1016/j.chemgeo.2014.09.023>, 2014.
- Palache, C., Clifford, F., and Berman, H.: *The System of Mineralogy*, John Wiley and Sons, 1963.
- [Rahl, J., Reiners, P. W., Campbell, I. H., Nicolescu, S., and Allen, C. M.: Combined single-grain \(U-Th\)/He and U/Pb dating of detrital zircons from the Navajo Sandstone, Utah." \*Geology\* 31.9 \(2003\): 761-764., \*Geology\*, 31, 761–764, 2003.](#)

Deleted: In press.

- Reiners, P. W. and Farley, K. A.: Influence of crystal size on apatite (U–Th)/He thermochronology: an example from the Bighorn Mountains, Wyoming, *Earth Planet. Sci. Lett.*, 188, 413–420, [https://doi.org/10.1016/S0012-821X\(01\)00341-7](https://doi.org/10.1016/S0012-821X(01)00341-7), 2001.
- 675 Reiners, P. W., Thomson, S. N., McPhillips, D., Donelick, R. A., and Roering, J. J.: Wildfire thermochronology and the fate and transport of apatite in hillslope and fluvial environments, *J. Geophys. Res. Earth Surf.*, 112, <https://doi.org/10.1029/2007JF000759>, 2007.
- Reiners, P. W., Carlson, R. W., Renne, P. R., Cooper, K. M., Granger, D. E., McLean, N. M., and Schoene, B.: *Geochronology and Thermochronology*, Wiley, 2018.
- 680 Spiegel, C., Kohn, B., Belton, D., Berner, Z., and Gleadow, A.: Apatite (U–Th–Sm)/He thermochronology of rapidly cooled samples: The effect of He implantation, *Earth Planet. Sci. Lett.*, 285, 105–114, <https://doi.org/10.1016/j.epsl.2009.05.045>, 2009.
- Thomson, Stuart N., Peter W. Reiners, John He, Sidney R. Hemming, and Kathy Licht: New constraints on the pre-glacial and glacial uplift and incision history of the central Transantarctic Mountains using multiple low-temperature thermochronometers, AGU Fall Meeting Abstracts, Vol. 2019, C14B-04, <https://ui.adsabs.harvard.edu/abs/2019AGUFM.C14B.04T/abstract>, 2019.
- 685 [Thomson, S. N., Reiners, P. W., Hemming, S. R., and Gehrels, G. E.: The contribution of glacial erosion to shaping the hidden landscape of East Antarctica, \*Nat. Geosci.\*, 6, 203–207, <https://doi.org/10.1038/ngeo1722>, 2013.](https://doi.org/10.1038/ngeo1722)
- 690 Whipp, D. M., Kellett, D. A., Coutand, I., and Ketcham, R. A.: Short communication: Modeling competing effects of cooling rate, grain size, and radiation damage in low-temperature thermochronometers, 4, 143–152, <https://doi.org/10.5194/gchron-4-143-2022>, 2022.
- Wolf, R. A., Farley, K. A., and Kass, D. M.: Modeling of the temperature sensitivity of the apatite (U–Th)/He thermochronometer, *Chem. Geol.*, 148, 105–114, [https://doi.org/10.1016/S0009-2541\(98\)00024-2](https://doi.org/10.1016/S0009-2541(98)00024-2), 1998.
- 695 Zeitler, P. K., Herczeg, A. L., McDougall, I., and Honda, M.: U–Th–He dating of apatite: A potential thermochronometer, *Geochim. Cosmochim. Acta*, 51, 2865–2868, [https://doi.org/10.1016/0016-7037\(87\)90164-5](https://doi.org/10.1016/0016-7037(87)90164-5), 1987.
- Ziegler, J. F.: Helium: Stopping powers and ranges in all elemental matter., 4, 1977.

Deleted: .

Deleted: .

We assume uniform spatial distribution of the parent nuclide, and apply both protocols to all fragments as we would in routine laboratory analyses: i.e. we assume no knowledge of the original length and thermal history of the crystals to compute the corrected age. Only the length and width of the broken crystals, and the number of terminations present, are used for the calculation.

Though the new  $F_T$  correction for broken crystals is more accurate as a whole than the old correction, the two ideal assumptions of the simple geometric argument above introduce additional uncertainty.

Finally

For larger datasets, especially in the case of larger-n analyses, this contributes to our understanding of the expected distribution of corrected dates from any given sample (Fig. 7) (He et al., 2021)

A future step towards a more rigorous evaluation of the uncertainty of individual-grain analyses or samples as a whole could involve the propagation of each of these uncertainties to account for sample and grain specific information such as the probability of implantation (approximated from the spatial distribution of heavy minerals in a sample, via XRCTX-Ray Computed Tomography), the probability of extreme parent nuclide zonations in a sample (based on fission track mounts) or from a reference compilation, and whether fragments were analyzed.